

# Functional Synthesis of a New Class of Micro Electro-Mechanical Systems

Nicola Pio Belfiore

Sapienza University of Rome,  
Department of Mechanical and Aerospace Engineering,  
via Eudossiana, 18, 00184 Rome, Italy  
nicolapio.belfiore@uniroma1.it  
<http://dima.uniroma1.it/belfiore/>

**Abstract.** This paper discloses a new method of functional synthesis of a new class of MEMS (Micro Electro-Mechanical Systems) that could be conceived thanks to: (a) a new concept flexural hinge (that has been recently patented by the Author) and (b) the accurate detection of a MEMS device pseudo-rigid-body equivalent mechanism, which allows the application of several classic algorithms well known in kinematic synthesis. The adopted approach is explained and two examples are presented. Finally, basic information is provided for the MEMS technology based construction process that has been used for prototyping.

**Keywords:** MEMS, kinematic synthesis, functional design, micro robotics.

## 1 Introduction

During the last decades MEMS devices have been increasingly employed for many purposes, such as, for example, accelerometers, gyroscopes, inkjet printers, pressure sensors, microphones, switching, energy harvesting, drug delivery systems, and many other types of sensors and actuators [1–11]. More recently, a new flexural hinge has been proposed for the design of MEMS [12–17], which discloses how to build a new class of multi Degrees of Freedom (DOF) MEMS devices. However, there are still many issues to be investigated such as, for example, the construction methods, the geometric optimization, the overall compliance characterization and control [18, 19] and, mainly, the design method, which the present paper is dedicated to. MEMS and compliant mechanisms are similar in many aspects since they can move because they are both composed of flexible (thinner) and pseudo-rigid (thicker) subparts. Therefore, all the methods developed for the study of the compliant mechanisms can be adopted for the study of MEMS devices. Thanks to some important papers presented in literature, such as, for example, Howell's and Midha's [20–23], the pseudo-rigid-body model has been introduced and refined to simulate a compliant mechanism for many types of geometry and loadings. The main advantage of using the pseudo-rigid-body equivalent mechanism consists in the fact that it can be analyzed as an ordinary

mechanism with revolute joints and therefore many different approaches can be used for topological [24–26] and kinematic higher order [27, 28] synthesis.

## 2 Theoretical Basis

The overall motion of MEMS devices can be understood only if the relative motion between any pair of adjacent *pseudo-rigid* links is identified. Unfortunately, this relative motion is not easy to figure out because it depends not only on geometry, but also on the intensity of the load which inflects the compliant parts. There are some basic strategies developed in order to set up the *most reliable* pseudo-rigid body model of a given compliant mechanism: the simplest one consists in substituting a flexible sub-part, connecting pseudo-rigid bodies  $i$  and  $j$ , by a revolute joint  $R$  whose center is positioned in correspondence of the center  $C_R$  of the finite relative rotation between pseudo-rigid links  $i$  and  $j$ . However, flexible parts have been simulated also by using two RR or even three RRR revolute joints. In the present investigation one single  $R$ , revolute joint, substitution is considered, because RR and RRR substitutions make the equivalent mechanism very impractical for the application of the kinematic synthesis methods and they introduce a great number of idle DOF.

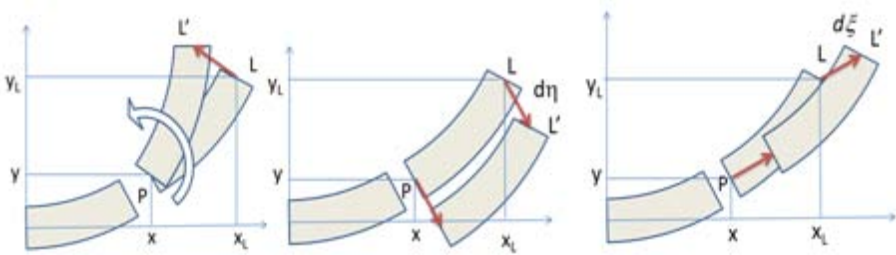


**Fig. 1.** Displacement of the end section center  $L$  due to the moment (a), shear (b) and normal tension (c) in the elementary section  $P$

Considering that the flexible sub-parts often consist of linear or curved beams, a pre-liminary analysis has been performed in order to ascertain where center  $CR$  could be positioned to.

### 2.1 Approximate Calculation of the Center $C_R$ of the Relative Rotation

A curved beam has been analyzed herein by assuming that: (a) the Hooke's Law holds for the material, (b) the external forces act in the plane which contains the curved beam axis; (c) the inflection axis is always normal to this plane;

(d) the material is isotropic and homogeneous. According to the Euler-Bernoulli static beam equation, given a torque  $M_k$  applied to the end section of a curved beam, the end section overall rotation  $\Delta\vartheta$  from the initial  $A_0B_0$  to the final  $A_kB_k$  position, is obtained by summing the infinitesimal rotations due to the deformations of all the elements along the curved axis  $s$ , from  $s = 0$  (framed section) to  $s = L$  (end section):

$$\Delta\vartheta = - \int_0^L \frac{M ds}{EI}, \quad (1)$$

where  $M$  is the bending moment in the beam,  $E$  is the elastic modulus and  $I$  is the second moment of area of the beam cross-section. With reference to Fig. 1, the end section displacement  $LL'$  from its initial position  $A_0B_0$  to its final position  $A_kB_k$  can be represented by the displacements  $\Delta x$  and  $\Delta y$  of the end section midpoint  $L$ . The latter are obtained by summing up the contributions due to tensile/compressive force  $N$ , Fig. 1(c), shear force  $T$ , Fig. 1(b), and to the bending moment  $M$ , Fig. 1(a), in all the cross-section elements in the beam, from  $s = 0$  to  $s = L$ , namely,

$$\Delta x = \int_0^L \frac{M ds}{EI} (y_L - y) + \int_0^L \frac{N dx}{EA} + \int_0^L \chi \frac{T dy}{GA}, \quad (2)$$

$$\Delta y = - \int_0^L \frac{M ds}{EI} (x_L - x) + \int_0^L \frac{N dy}{EA} - \int_0^L \chi \frac{T dx}{GA}, \quad (3)$$

where  $G$  is the shear modulus,  $A$  is the beam cross-section area, and  $\chi > 1$  is a shear correction factor introduced in order to allow the non-uniform shear strain to be expressed as a constant. Eqns. (1)–(3) can be used to obtain the positions  $A_kB_k$  of the beam end section for increasing values of the external torque  $M_{k+1} > M_k$ , as reported in Fig. 2. By using the theory of displacement matrices, as for example in [17], the coordinates  $x_{0k}$  and  $y_{0k}$  of the center of the finite rotation of the end-section from the initial position to the  $k$ -th one can be expressed as the functions

$$x_{0k} = x_L + \frac{\Delta x}{2} - \Delta y \frac{\sin(\Delta\vartheta)}{2(1 - \cos(\Delta\vartheta))} \quad (4)$$

$$y_{0k} = y_L + \frac{\Delta y}{2} + \Delta x \frac{\sin(\Delta\vartheta)}{2(1 - \cos(\Delta\vartheta))} \quad (5)$$

of  $\Delta\vartheta$ ,  $\Delta x$  and  $\Delta y$ . Fig. 2 shows the positions of 4 finite rotation centers. By iterating the procedure 20 times, it could be ascertained that the less the module of the externally applied moment  $M_k$ , the more the corresponding center  $C_{0k}$  gets close to the center  $C$  of the elastic weights of the beam. Such result suggests the idea of creating the pseudo-rigid body model by substituting, in the compliant mechanism, any elastic beam by a revolute joint  $R$  positioned in correspondence of the center of the elastic weights of the beam.

## 2.2 Kinematic Synthesis of the PRB Equivalent Mechanism

By using the results obtained in the previous paragraph, the development of new MEMS devices can be based on the adoption of a pseudo-rigid-body (PRB for short) mechanism which is obtained by introducing, for each elastic joint (flexible curved beam), one revolute joint R whose center is placed in correspondence of the center of the elastic weights of the flexible beam. This method is simpler and also more accurate than those which use, for each elastic joint, two RR or even three RRR revolute joints [29, 30].

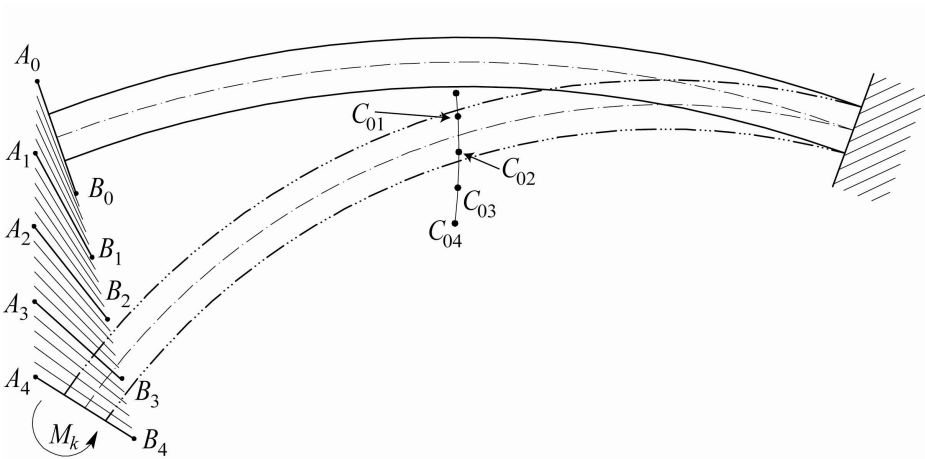


**Fig. 2.** Displacements  $A_kB_k$  of the end section  $A_0B_0$  of a curved beam subject to incremental torques  $M_k$  and their correspondent centers of the relative motions  $C_{0k}$ , with  $k = 1, 2, 3, 4$

The correspondence between *compliant mechanisms* and *PRB models* is not a bijective function because obtaining a PRB mechanism starting from a compliant mechanism is, intrinsically, an approximate procedure. In fact, since the centers of the relative motions between adjacent links depend on the applied loads, generally it doesn't exist a unique *PRB model* which is able to substitute the original *compliant mechanism* without errors in motion reproduction. Hence, for a given compliant mechanism there are many PRB models which simulate the motion, but they all will do that *approximately*. Analogously, the *inverse* process of building a compliant mechanism (MEMS device) starting from a *PRB mechanism* will not admit a unique solution and there will be, generally, several solutions which can be generated. By using this inverse approach, it is possible to use type [31] and kinematic synthesis.

Three main classic problems of kinematic synthesis have been investigated in the past century, namely, rigid body guidance, function generator and path generator. Except for the first, they can be studied both for finite and infinitesimal

motion, and, so, a large variety of applications has been developed for many purposes. As far as MEMS devices are concerned, the limited mobility around the neutral configuration suggests the idea that infinitesimal motion could be the preferred theoretical back-ground. However, as shown in previous works [12–16], silicon allows an unexpectedly large inflection and so the new silicon flexural hinges, embedded in the new class of MEMS, offer a range of relative rotations approximately equal to  $[-20^\circ, +20^\circ]$ . Therefore, it is not convenient to exclude the class of algorithms explicitly conceived for the finite displacements. The Author has attempted to give an estimation of the attitude of the main classes of algorithms used in kinematic synthesis to yield promising results in MEMS design and such assessment is resumed in Table 1.

**Table 1.** A rough estimation (2014) of all the possible applications of the methods developed in Kinematic Synthesis to MEMS design and optimization

<b>MEMS Synthesis</b>	<b>Function generator</b>	<b>Path generator</b>	<b>Rigid Body Guidance</b>
Finite motion	<i>very promising</i>	<i>very promising</i>	<i>Promising</i>
Infinitesimal motion	<i>rare applications</i>	<i>very promising</i>	<i>Unpractical</i>

In the following paragraphs it will be shown how the synthesis of a PRB mechanism can be done by using classic approaches in kinematic synthesis, such as Burmester’s and Generalized Burmester’s Theory [32], Freudenstein’s equation, and Suh’s and Radcliffe’s Displacement Matrices Synthesis [33] for finite motions.

### 3 Design Method

Once a method to establish a reliable, although approximate, compliant-to-PRB mechanism correspondence is chosen, the whole design approach can be based on classic design steps. Hence, provided that the procedure based on single R substitution of the compliant beams, as described in paragraphs 2.1 and 2.2, is accepted, the following steps can be adopted.

1. Number and Type synthesis of the PRB mechanism
2. Kinematic Synthesis of the PRB mechanism
3. Construction of the real *compliant mechanism (MEMS device)* from the PRB mechanism
4. Kinetostatic Validation via FEA and/or theoretical modeling
5. Prototyping and experimental validation

In the following paragraph, Steps 2, 3 and 5 will be exemplified.

## 4 Examples of Application

In this paragraph two examples of applications are considered. As a first case study, the kinematic synthesis of a 3 DOF parallel plane [34] platform for finite displacements is considered, for three assigned orientations of the mobile platform. The second case study consists in the synthesis of a mechanism which generates a circular arc with the fourth order of approximation in the neighborhood of a coupler point. For this problem the class of algorithms dedicated to infinitesimal motion is considered [35].

### 4.1 Function Generator for Finite Displacements

With reference to Fig. 3, the design goal is supposed to be the synthesis of a parallel micro-robot with three prescribed platform angular positions  $\psi_1$ ,  $\psi_2$ , and  $\psi_3$  for three corresponding prescribed angular positions of an input link  $\varphi_1$ ,  $\varphi_2$ , and  $\varphi_3$ , assuming that the platform tip  $M$  had null displacements. Assuming also that the parallel platform is supported by two symmetric binary legs, symbols  $a$  and  $b$  will stand for the lengths of the leg links, while  $c$  will represent the half length of the upper platform link.

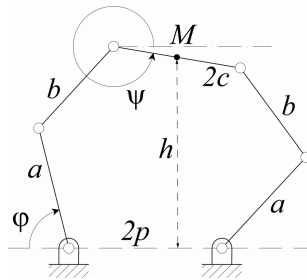


**Fig. 3.** Nomenclature

While the frame link length  $2p$  and the platform tip  $M$  height  $h$  (with respect to the frame link) are supposed to be known parameters, the lengths  $a$ ,  $b$ , and  $c$  are unknown. Hence, the synthesis of a function generator mechanism consists in finding the unknown lengths in such a way that the three pairs of angles  $(\varphi_1, \psi_1)$ ,  $(\varphi_2, \psi_2)$ , and  $(\varphi_3, \psi_3)$  hold for three configurations.

**Application of the Freudenstein's Equation.** According to the Nomenclature defined in Fig. 3 and to the assumed requirements, it is possible to consider the tip point  $M$  as a fixed point in the plane, since only the rotations are inquired, and, so, the distance between the first revolute joint and point  $M$  remains positioned as in the undeformed neutral configuration. As shown in Fig. 4(a) this

distance will be referred to as  $d = \sqrt{h^2 + p^2}$ , where  $h$  is the point  $M$  height with respect to the frame link and  $p$  is the frame link half-length. According to the Figure, angle  $\chi$  can be easily obtained from the system geometry, being  $\frac{h}{p} = \tan \chi$ .

Since three pairs of angles  $\varphi$  and  $\psi$  are given, the following system of equations can be written

$$\begin{cases} R_1 \cos \varphi_i - R_2 \cos \psi_i + R_3 = \cos(\varphi_i - \psi_i) \\ i = 1, 2, 3 \end{cases} \quad (6)$$

and solved with respect to  $R_1$ ,  $R_2$  and  $R_3$ . Since  $d$  is known, the unknown variables of the problem can be obtained:

$$\begin{cases} c = \frac{d}{R_1} \\ a = \frac{d}{R_2} \\ b^2 = a^2 + c^2 + d^2 - 2acR_3 \end{cases} \quad (7)$$

**Table 2.** Dimensions  $a$ ,  $b$  and  $c$  of the links, as obtained by applying the Freudenstein’s equation for the prescribed set of input and output angles

Input angles			Output angles			Link dimensions ( $\mu\text{m}$ )		
$\varphi_1$	$\varphi_2$	$\varphi_3$	$\psi_1$	$\psi_2$	$\psi_3$	$a$	$b$	$c$
$105^\circ$	$115^\circ$	$135^\circ$	$37^\circ$	$59^\circ$	$81^\circ$	27	36	22

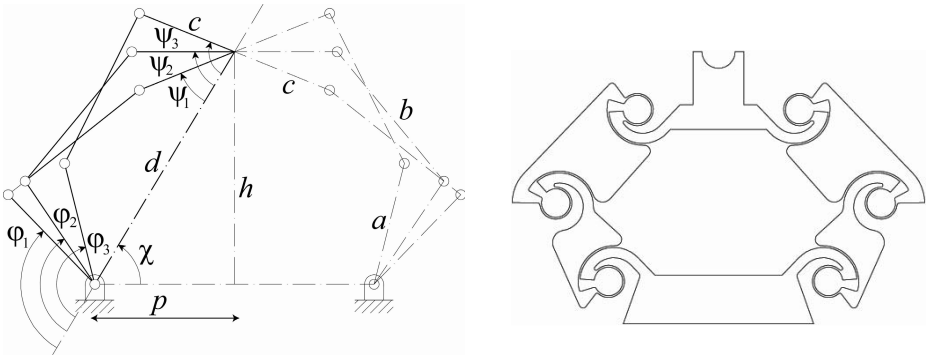


**Fig. 4.** Application of the Freudenstein’s equation to the synthesis of a four-bar linkage function generator (a) embedded in a planar MEMS technology based 3 DOF platform (b)

**Numerical Results.** A representative example of application of the general method based on the Freudenstein's equation for the generation of a function generation four-bar linkage is reported herein. Given the frame link half-length  $p = 30 \mu\text{m}$  and the undeformed platform height  $h = 50 \mu\text{m}$ , Freudenstein's equation could be applied to a *virtual* four-bar linkage  $a$ ,  $b$ ,  $c$  and  $d$  which works as a function generator (for three prescribed pairs of  $\varphi$  and  $\psi$  angles) embedded *inside* the kinematic structure of the parallel platform. Fig. 4(a) displays pictorially the idea of embedding a four-bar linkage in the parallel mechanism and it reports the adopted nomenclature and symbols. The numerical values are summarized in Table 2.

**Deduction of the Real MEMS Device and Prototyping.** Starting from the PRB mechanism that has been obtained by using Freudenstein's equation, a *real* compliant mechanism (or MEMS) can be built, for example, as the one depicted in Fig. 4(b). Fig. 5 shows a detail of a sample from the family of the silicon micro-robots prototypes that have been manufactured via Reactive-Ion Etching RIE process and that are based on the new flexural hinge [36, 37].

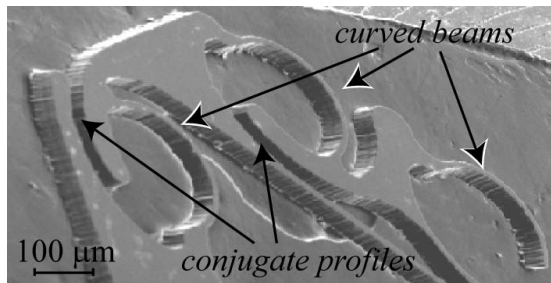


**Fig. 5.** A SEM (Scanning Electron Microscope) detailed view of three flexural hinge of a silicon microrobot

In Fig. 5 three silicon flexural hinges, each one being composed of a flexible curved beam and a pair of conjugate profiles, are represented by means of a SEM image. This MEMS device has been obtained by means of a  $50 \mu\text{m}$  depth RIE Etching.

#### 4.2 Kinematic Synthesis of Path Generator Mechanism for Infinitesimal Motion

As a second case study the kinematic synthesis of a path generator mechanism for infinitesimal motion is considered. A circular arc is considered as the prescribed path and a fourth order accuracy is required for the approximating coupler curve.



**Application of the Classic Burmester's Theory.** Among the variety of methods for the kinematic synthesis of mechanisms, those based on the geometric invariants have been used in many applications. The geometric invariants  $a(\varphi)$  and  $b(\varphi)$  are introduced as the coordinates of the origin of the Canonic Reference System attached to the mobile plane with respect to the fixed (absolute) reference frame. Both coordinates are regarded as a function of the angular position of the mobile reference frame and their first  $a_1, b_1$  and higher order derivatives  $a_2, b_2, \dots, a_n, b_n$ , with respect to  $\varphi$  are introduced as *geometric invariants*. The first, second, third and fourth order derivatives have the meaning of the *geometric velocity, acceleration, jerk* and *jounce* of the origin of the mobile reference system. By introducing the Canonic Reference System  $(C, \xi, \eta)$ , which has the origin positioned in correspondence of the instantaneous center of rotations  $C$ , and the axes  $\xi$  and  $\eta$  tangent and orthogonal, respectively, to the *centrodes* in  $C$ , the expression of the *cubic of stationary curvature* can be expressed in a simplified form

$$(\xi^2 + \eta^2)(\xi a_3 + \eta b_3) + 3\xi b_2(\xi^2 + \eta^2 - b_2\eta) = 0. \quad (8)$$

Eqn. (8) represents the locus of points (of the mobile plane) for which the trajectory has a stationary curvature radius. The Burmester's points can be found by solving the system of equations composed of Eqn. (8) and of the stationary condition for the second order derivative

$$\frac{d^2\kappa}{d\varphi^2} = 0 \quad (9)$$

of the curvature  $\kappa = \frac{d\varphi}{ds}$ , where  $s$  is the scalar abscissae along the trajectory. Although the locus defined by Eqn. (9) has no interesting meaning, this condition, if taken together with condition (8), defines a discrete number of points whose trajectory describes an arc of circle with fourth order approximation.

**Table 3.** Numerical values for the crank, coupler, rocker and frame link lengths, crank angle and coordinates of one Burmester's point

Independent design variables					Output variables		
Crank length	Coupler length	Rocker length	Frame link length	Crank angle	$B_x$	$B_y$	curvature radius
45 $\mu\text{m}$	140 $\mu\text{m}$	200 $\mu\text{m}$	260 $\mu\text{m}$	70°	-277 $\mu\text{m}$	282 $\mu\text{m}$	1.7 mm

For the set of data given in Table 3, which includes the lengths of the crank  $DL$ , coupler  $LE$ , rocker  $EM$ , frame  $DM$  and the given crank angle with respect to the frame, one feasible Burmester's point could be found by solving the system of equations (8) and (9). The path of  $B$ , attached to the coupler, does approximate a circular arc with a fourth order approximation. Point  $B$  coordinates and the trajectory curvature radius are given also in Table 3.

**Construction of the Real Device.** Starting from the given four-bar linkage and using the position of point B, a path generator MEMS device could be built by means of single R substitution. Each revolute joint R of the resultant four-bar linkage has been substituted by a new concept flexural hinge. As shown in Fig. 7, point B must be attached to the pseudo-rigid coupler link.

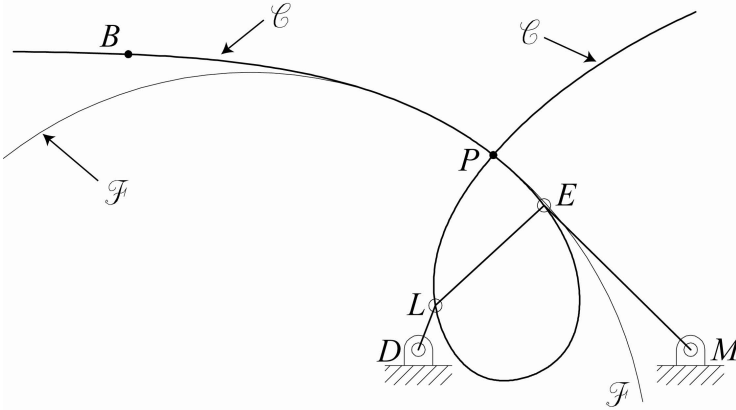


**Fig. 6.** Detection of the inflexion circle  $\mathcal{F}$ , the cubic of stationary curvature curve  $\mathcal{C}$  and of point B, which is one of the Burmester's point

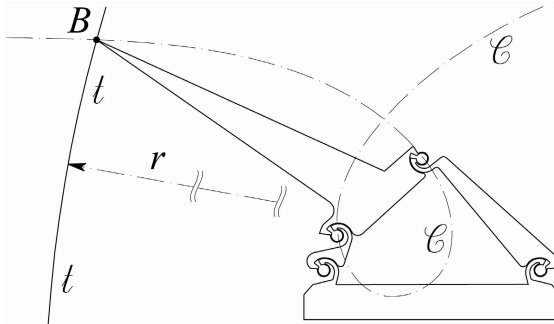


**Fig. 7.** The MEMS technology based silicon micro four bar linkage generating the circular arc  $t$  ( $r$  being the radius) in the neighborhood of point B, which is one of the Burmester's point

## 5 Conclusions

In this paper, firstly the inflexion of a generic curved beam has been analyzed by means of Euler Bernoulli element model: the study of the relative displacements among the beam extreme sections showed how to build a method, based on single revolute joint R substitution, for detecting a feasible *pseudo rigid body mechanism* which could be considered as the equivalent of a given *compliant*

*mechanism*. Then, the idea of applying kinematic synthesis to MEMS design, via R substitution, has been explained and two examples have been presented: function generation for finite displacements by means of Freudenstein's equation and path generation for infinitesimal motion by means of the classic Burmester's theory. For each problem, one possible MEMS device has been presented. Prototypes could be obtained by using Reactive Ion Etching (RIE) process. The whole method relies on the use of a new concept flexural hinge that has been recently patented by the Author.

## References

1. Nguyen, N.-T., Huang, X., Chuan, T.K.: MEMS-micropumps: A review. *Journal of Fluids Engineering, Transactions of the ASME* 124(2), 384–392 (2002)
2. Cook-Chennault, K.A., Thambi, N., Sastry, A.M.: Powering MEMS portable devices - A review of non-regenerative and regenerative power supply systems with special emphasis on piezoelectric energy harvesting systems. *Smart Materials and Structures* 17(4), art. no. 043001 (2008)
3. Grayson, A.C.R., Shawgo, R.S., Johnson, A.M., Flynn, N.T., Li, Y., Cima, M.J., Langer, R.: A BioMEMS review: MEMS technology for physiologically integrated devices. *Proceedings of the IEEE* 92(1), 6–21 (2004)
4. Ho, C.-M., Tai, Y.-C.: Review: MEMS and its applications for flow control. *Journal of Fluids Engineering, Transactions of the ASME* 118(3), 437–447 (1996)
5. Tsai, N.-C., Sue, C.-Y.: Review of MEMS-based drug delivery and dosing systems. *Sensors and Actuators, A: Physical* 134(2), 555–564 (2007)
6. Tanaka, M.: An industrial and applied review of new MEMS devices features. *Micro-electronic Engineering* 84(5-8), 1341–1344 (2007)
7. Chuang, W.-C., Lee, H.-L., Chang, P.-Z., Hu, Y.-C.: Review on the modeling of electrostatic MEMS. *Sensors* 10(6), 6149–6171 (2010)
8. Tekin, T.: Review of packaging of optoelectronic, photonic, and MEMS components. *IEEE Journal on Selected Topics in Quantum Electronics* 17(3), art. no. 5740939, 704–719 (2011)
9. Jones, B.E., Yan, T.: MEMS force and torque sensors/a review. *Measurement and Control* 37(8), 236–241 (2004)
10. Bogue, R.: Recent developments in MEMS sensors: A review of applications, markets and technologies. *Sensor Review* 33(4), art. no. 17094935, 300–304 (2013)
11. Nenzi, P., Crescenzi, R., Dolgyi, A., Klyshko, A., Bondarenko, V., Belfiore, N.P., Balucani, M.: High density compliant contacting technology for integrated high power modules in automotive applications. In: *Proceedings - Electronic Components and Technology Conference*, art. no. 6249111, pp. 1976–1983 (2012)
12. Belfiore, N.P., Verotti, M., Crescenzi, R., Balucani, M.: Design, optimization and construction of MEMS-based micro grippers for cell manipulation. In: *Proceedings of the ICSSE 2013 - IEEE International Conference on System Science and Engineering*, art. no. 6614642, pp. 105–110 (2013)
13. Belfiore, N.P., Emamimeibodi, M., Verotti, M., Crescenzi, R., Balucani, M., Nenzi, P.: Kinetostatic optimization of a MEMS-based compliant 3 DOF plane parallel platform. In: *Proceedings of the ICCS 2013 - IEEE 9th International Conference on Computational Cybernetics*, art. no. 6617600, pp. 261–266 (2013)

14. Belfiore, N.P., Balucani, M., Crescenzi, R., Verotti, M.: Performance analysis of compliant MEMS parallel robots through pseudo-rigid-body model synthesis. In: ASME 2012 11th Biennial Conference on Engineering Systems Design and Analysis, ESDA 2012, vol. 3, pp. 329–334 (2012)
15. Balucani, M., Belfiore, N.P., Crescenzi, R., Genua, M., Verotti, M.: Developing and modeling a plane 3 DOF compliant micromanipulator by means of a dedicated MBS code. In: Technical Proceedings of the 2011 NSTI Nanotechnology Conference and Expo, NSTI-Nanotech 2011, vol. 2, pp. 659–662 (2011)
16. Balucani, M., Belfiore, N.P., Crescenzi, R., Verotti, M.: The development of a MEMS/NEMS-based 3 D.O.F. compliant micro robot. In: Proceedings of the 19th International Workshop on Robotics in Alpe-Adria-Danube Region, RAAD 2010, art. no. 5524590, pp. 173–179 (2010)
17. Belfiore, N.P., Simeone, P.: Inverse kinetostatic analysis of compliant four-bar linkages. *Mechanism and Machine Theory* 69, 350–372 (2013)
18. Belfiore, N.P., Verotti, M., Di Giamberardino, P., Rudas, I.J.: Active Joint Stiffness Regulation to Achieve Isotropic Compliance in the Euclidean Space. *Journal of Mechanisms and Robotics* 4(4), art. no. 041010 (2012)
19. Belfiore, N.P., Di Giamberardino, P., Rudas, I.J., Verotti, M.: Isotropy in any RR planar dyad under active joint stiffness regulation. In: Proceedings of the 19th International Workshop on Robotics in Alpe-Adria-Danube Region, RAAD 2010, art. no. 5524581, pp. 219–224 (2010)
20. Howell, L.L., Midha, A., Norton, T.W.: Evaluation of equivalent spring stiffness for use in a pseudo-rigid-body model of large-deflection compliant mechanisms. *Journal of Mechanical Design, Transactions of the ASME* 118(1), 126–131 (1996)
21. Yu, Y.-Q., Howell, L.L., Lusk, C., Yue, Y., He, M.-G.: Dynamic modeling of compliant mechanisms based on the pseudo-rigid-body model. *Journal of Mechanical Design, Transactions of the ASME* 127(4), 760–765 (2005)
22. Midha, A., Howell, L.L., Norton, T.W.: Limit positions of compliant mechanisms using the pseudo-rigid-body model concept. *Mechanism and Machine Theory* 35(1), 99–115 (2000)
23. Edwards, B.T., Jensen, B.D., Howell, L.L.: A pseudo-rigid-body model for initially-curved pinned-pinned segments used in compliant mechanisms. *Journal of Mechanical Design, Transactions of the ASME* 123(3), 464–468 (2001)
24. Belfiore, N.P.: Distributed Databases for the development of Mechanisms Topology. *Mechanism and Machine Theory* 35(12), 1727–1744 (2000)
25. Belfiore, N.P.: Atlas of remote actuated bevel gear wrist mechanisms of up to nine links. *International Journal of Robotics Research* 12(5), 448–459 (1993)
26. Belfiore, N.P., Pennestr, E.: An atlas of linkage-type robotic grippers. *Mechanism and Machine Theory* 32(7), 811–833 (1997)
27. Pennestri, E., Belfiore, N.P.: On the numerical computation of Generalized Burmester Points. *Meccanica* 30(2), 147–153 (1995)
28. Pennestri, E., Belfiore, N.P.: Modular third-order analysis of planar linkages with applications. American Society of Mechanical Engineers, Design Engineering Division (Publication) DE 70(pt. 1), 99–103 (1994)
29. Yu, Y.-Q., Feng, Z.-L., Xu, Q.-P.: A pseudo-rigid-body 2R model of flexural beam in compliant mechanisms. *Mechanism and Machine Theory* 55, 18–33 (2012)
30. Chen, G., Xiong, B., Huang, X.: Finding the optimal characteristic parameters for 3R pseudo-rigid-body model using an improved particle swarm optimizer. *Precision Engineering* 35(3), 505–511 (2011)

31. Her, I., Midha, A.: Compliance Number Concept for compliant mechanisms and Type Synthesis. *Journal of Mechanisms, Transmissions, and Automation in Design* 109(3), 348–355 (1987)
32. Freudenstein, F., Bottema, O., Koetsier, M.T.: Finite conic-section Burmester Theory. *Journal of Mechanisms* 4(4), 359–373 (1969)
33. Suh, C.H., Radcliffe, C.W.: Synthesis of Plane Linkages With Use of the Displacement Matrix. *J. Eng. Ind.* 89(2), 206–214 (1967)
34. Belfiore, N.P.: Brief note on the concept of planarity for kinematic chains. *Mechanism and Machine Theory* 35(12), 1745–1750 (2000)
35. Di Benedetto, A., Pennestrò, E.: Introduction to mechanism kinematics, vol. 1, 2 & 3. Casa Editrice Ambrosiana, Milano (1993-1999) (in Italian)
36. Belfiore, N.P., Scaccia, M., Ianniello, F., Presta, M.: Selective compliance hinge. US Patent 8,191,204, WO2009034551A1 (2012)
37. Belfiore, N.P., Ianniello, F., Perfetti, L., Presta, M., Scaccia, M.: Selective compliance wire actuated mobile platform, particularly for endoscopic surgical devices. US Patent US 20110028988 A1, WO 2009034552 A3 (2009)